HHS Public Access

Author manuscript

Sci Signal. Author manuscript; available in PMC 2019 May 08.

Published in final edited form as:

Sci Signal. ; 11(529): . doi:10.1126/scisignal.aao1815.

Chemical synapses without synaptic vesicles: purinergic neurotransmission via a CALHM1 channel-mitochondrial signaling complex

Roman A. Romanov[1,2,3], **Robert S. Lasher**[4], **Brigit High**[4], **Logan E. Savidge**[4], **Adam Lawson**[4], **Olga A. Rogachevskaja**[1], **Haitian Zhao**[5], **Vadim V. Rogachevsky**[1], **Marina F. Bystrova**[1], **Gleb D. Churbanov**[1], **Igor Adameyko**[6,7], **Tibor Harkany**[2,7], **Ruibiao Yang**[4], **Grahame J. Kidd**[8], **Philippe Marambaud**[5], **John C. Kinnamon**[9], **Stanislav S. Kolesnikov**[1,*], and **Thomas E. Finger**[4,*]

[1]Institute of Cell Biophysics RAS, Pushchino, Moscow region, 142290, Russia

[2]Department of Molecular Neurosciences, Center for Brain Research, Medical University of Vienna, A-1090 Vienna, Austria

[3]Immanuel Kant Baltic Federal University, Kaliningrad, 236041, Russia

[4]Rocky Mountain Taste & Smell Center, Dept. Cell & Developmental Biology, University Colorado School of Medicine, Aurora, CO 80045, USA

[5]Litwin-Zucker Research Center for the Study of Alzheimer's Disease, The Feinstein Institute for Medical Research, Manhasset, NY, 11030, USA

[6]Department of Physiology and Pharmacology, Karolinska Institutet, SE-17177 Stockholm, Sweden

[7]Department of Neuroscience, Karolinska Institutet, SE-17177 Stockholm, Sweden

[8]Department of Neuroscience, Lerner Research Institute, Cleveland Clinic, Cleveland, OH, 44195, USA

[9]Rocky Mountain Taste & Smell Center, Dept. Biological Sciences, University of Denver, Denver, CO 80210, USA

Abstract

[*]Correspondence to: Thomas E. Finger, tom.finger@ucdenver.edu.
[*]Co-senior authors.
Correspondence and requests for materials should be addressed to Roman Romanov roman.romanov@meduniwien.ac.at or Thomas Finger tom.finger@ucdenver.edu.

Author Contribution: S.S.K. T.E.F. and R.A.R. designed the study; R.A.R., T.E.F., and R.Y. performed immunostaining; R.A.R., performed calcium imaging and electrophysiological experiments, R.A.R., O.A.R.; M.F.B. performed experiments with cellular ATP and ATP/ADP sensors; H.Z. and P.M. developed and characterized the antibody against CALHM1; V.V.R., T.E.F., B.H., R.S.L., R.Y., L.E.S., G.K., A.L., J.C.K. performed electron microscopy experiments and made 3D-reconstructions; G.D.C. and O.A.R. performed experiments with effects of CBX; R.A.R., T.E.F., I.A., T.H., P.M. and S.S.K. analyzed data and contributed to writing the paper. All Authors commented on the manuscript and approved its submission.

Competing Interests: Authors declare no competing financial interests.

Data and Materials availability: n/A

Competing Intrests: none

The synapse linking taste receptor cells to the taste nerves shows unusual functional properties suggestive of a unique structural organization. Conventional chemical synapses in the nervous system involve a presynaptic accumulation of neurotransmitter-containing vesicles, which upon activation, fuse to the plasma membrane to release neurotransmitter that activates receptors on the postsynaptic cell. In taste buds, taste receptor cells (Type II sensory cells) exhibit no conventional synaptic features but nonetheless show regulated release of their afferent neurotransmitter, ATP -- not via fusion of synaptic vesicles to the membrane but rather through a large-pore, voltage-gated channel, CALHM1. Immunohistochemistry reveals that CALHM1 is tightly localized to points of contact between the receptor cells and sensory nerve fibers. Ultrastructural and super-resolution light microscopy show that the CALHM1 channels always are associated with distinctive, large (1–2μm) mitochondria spaced 20–40 nm from the presynaptic membrane. Pharmacological disruption of the mitochondrial respiratory chain limits the ability of the taste cells to release ATP suggesting that the immediate source of released ATP is the mitochondrion rather than a global cytoplasmic pool of ATP. These large mitochondria may serve as both a reservoir of releasable ATP as well as the site of synthesis. The juxtaposition of the large mitochondrion to the areas of membrane displaying CALHM1 also define a restricted compartment that limits the influx of Ca^{2+} upon opening of the non-selective CALHM1 channels. These findings reveal a distinctive organelle signature and functional organization for regulated, focal release of purinergic signals in the absence of synaptic vesicles.

INTRODUCTION

A synapse, defined originally in 1897 for the nervous system by Foster & Sherrington (1), is a point of cell-to-cell contact specialized for rapid signalling between cells. This term also has been applied to the signaling complex formed at the point of contact between T cells and antigen-presenting cells of the immune system (2). In the nervous system, synapses may be either electrical or chemical in nature. An electrical synapse involves physical contact between cell membranes enabling direct transmission of electrical signals between cells. Chemical synapses entail release of neurotransmitter by the presynaptic, signalling cell into a gap between the cells followed by activation of specific receptors on the postsynaptic cell to evoke a cellular response. In a conventional chemical synapse, the neurotransmitter molecules lie within synaptic vesicles, which fuse to the adjacent presynaptic membrane following Ca^{2+} influx. We describe here a different type of chemical synapse by which taste receptor cells signal to the sensory nerve fibers.

Taste buds, the sensory endorgans for gustation, comprise 50–80 specialized epithelial cells residing in distinctive papillae of the tongue and elsewhere in the oropharynx. When a taste substance stimulates the apices of the taste receptor cells, the cells release neurotransmitter onto the sensory nerve fibers innervating the taste bud. Previous studies (3, 4) have established that the key neurotransmitter released in this system is ATP since either pharmacological blockade or genetic deletion of the neural ATP receptors eliminates nearly all responses in the taste nerves (3–5). Consistent with the necessity for purinergic transmission in this system, all gustatory nerve fibers possess P2X-type purinergic receptors (6–8).

The functional contacts between taste cells and nerve fibers differ according to the type of taste cell involved. Type I taste cells are glia-like and display no specialized points of contact with nerve fibers (9) whereas Type III cells, which transduce sour (acid) and perhaps other ionic qualities (9–11), form conventional chemical synapses complete with voltage-gated Ca^{2+} channels (12, 13), pre- and post-synaptic membrane thickening, and synaptic vesicles with their associated SNARE complex proteins (14). In these features, Type III cells are similar to axonless receptor cells in other sensory systems, e.g. hair cells and photoreceptors. In contrast, Type II taste cells, which transduce sweet, umami, or bitter tastes, lack neuronal SNARE proteins and synaptic vesicles (12, 15) but nonetheless release ATP as a neurotransmitter in a regulated fashion (16–18). This output from Type II cells is unconventional because it does not involve the Ca^{2+}-dependent exocytosis of vesicles but relies on ATP release through voltage-gated ATP-permeable channels (16, 17). The transduction cascade in these taste cells begins with G-protein coupled receptors whose activation evokes release of Ca^{2+} from intracellular stores; the increases in Ca^{2+} triggers the transduction channel, TrpM5 (transient receptor potential cation channel subfamily M member 5), to initiate an action potential in the taste cells (9, 19). Recently, Taruno and collaborators (20) demonstrated that these action potentials trigger open the transmembrane protein Calcium Homeostasis Modulator 1 (CALHM1) which forms voltage-gated, ATP-permeable channels responsible for neurotransmission from Type II cells to the taste nerve. The channel-dependent ATP-release exhibits a steep dependence on membrane voltage with a threshold of about −10 mV (16, 21, 22). Accordingly, Type II taste cells, which generate action potentials much above the ATP-release threshold (20, 22), entrain afferent output reliably as a function of the magnitude of stimulation (18); see also (22) for discussion. Thus, similar to quantal release in classical synapses, neurotransmission in Type II taste cells is pulsatile since ATP release is driven by discrete action potentials (16, 18, 20). Although ATP-secretion is a common feature of a broad variety of other tissues utilizing purinergic autocrine/paracrine regulation, ATP-secretion in those systems, unlike taste buds, is long-lasting and continuous (23).

The CALHM1 channels underlying the ATP release from taste cells are large pore (≈ 14Å) (19, 20), slow-acting channels which accomodate outrush of ATP molecules as well as influx of numerous ionic species. Unclear, however is the distribution of these channels across the taste cell membrane. If widely distributed, opening of such large pore channels would permit wholesale influx of Ca^{2+} into the cells possibly triggering adverse events such as apoptosis. The ongoing functionality of the receptor cells, even after maximal activation, suggests that Ca^{2+} influx is somehow limited. We show that, unlike other channels implicated in taste transduction ((24), (25)), the CALHM1 channels are tightly restricted to points of contact with afferent nerve fibers. These points of contact between Type II taste cells and nerve fibers often exhibit large, so-called “atypical” mitochondria[1] with enlarged tubular cristae (7, 26). We investigated the possibility that these atypical mitochondria were closely associated with the CALHM1 channels thereby offering not only a source of ATP for release but also forming a restricted compartment for control of Ca^{2+} influx.

[1]We retain the term “atypical” as defined previously for this system (26) even while recognizing that mitochondria assume a variety of morphologies depending on their location and utilization. Mitochondria with tubular cristae also occur in diverse locations including photoreceptors and steroid-producing cells ((34)).

RESULTS

Ca^{++} flux and CALHM1 Channels

The main candidate for the release of ATP from taste cells is the recently discovered non-selective, large pore ion channel, CALHM1, with a pore size in excess of about 14Å (20). Being non-selective, the CALHM1 channel is permeable not only to ATP but also to a variety of ions, including Ca^{2+}. It therefore might be expected that appropriate depolarization of Type II cells should trigger global Ca^{2+} influx with concommitant rise in intracellular Ca^{2+}, as is the case following activation of Type III taste cells, which express voltage-gated Ca^{2+} channels but no CAHLM1 (27, 28). In our experiments, Type II taste cells, identified physiologically as those showing large, non-selective outward currents and ATP release upon depolarization (16, 21, 28), were assayed simultaneously with the patch clamp and Ca^{2+} imaging techniques (Fig. 1A). Surprisingly, depolarization-elicited ATP release was not always accompanied by marked increases in intracellular Ca^{2+}. Rather, of 40 Type II cells examined, 23 exhibited no evident change in cytoplasmic Ca^{2+} upon depolarization to 0 mV and higher (Fig. 1C). In the remaining 17 cells, depolarization elicited both robust ATP release (red trace in Fig. 1D) and detectable Ca^{2+} transients, which however were small and recovered to baseline within few seconds (black trace in Fig. 1D), suggesting them to be local.

Several findings point to CALHM1 as being responsible for the small Ca^{2+} transients observed in these depolarized Type II cells. First, in those cells showing a Ca^{2+} signal, the magnitude of the Ca^{2+} influx was proportional to the amount of ATP released (Fig. 1B; Suppl Table S1) suggesting these processes are regulated by a common mechanism. Second, these Ca^{2+} signals varied with bath Ca^{2+}, being abolished at zero Ca^{2+} and markedly increased at 10 mM Ca^{2+} (Fig. 1E). This demonstrated that Ca^{2+} influx rather than release from intracellular stores underlay the voltage-gated intracellular Ca^{2+} signals. In addition, CALHM1 is structurally related to the connexin and innexin family of channels all of which exhibit decreased conductance with low pH (29–31). We find that lowering extracellular pH from 7.2 to 5.8 decreases Ca^{2+} influx by about 50% (Fig. 1F). Finally, extracellular Gd^{3+} (100 μM), which inhibits various channels including CALHM1 (35), strongly decreased Ca^{2+} influx and CALHM-mediated voltage-gated outward currents in type II (taste cells (Fig. 1G). Taken together with previous findings, these results implicate CALHM1 in Ca^{2+} influx into Type II taste cells along with its previously demonstrated role in ATP efflux from these cells (19).

Why depolarization capable of driving a large ion current via CALHM channels resulted in a negligible Ca^{2+} signal in most Type II cells remained enigmatic. We hypothesized that Ca^{2+} influx might be limited by compartmentalization of CALHM channels into a signalling complex with an atypical mitochondrion, which could provide both space exclusion and mitochondrial Ca^{2+} uptake, thereby preventing the transformation of CALHM-mediated Ca^{2+} influx into a large and global Ca^{2+} transient. If this compartmentalization was the case, then mechanical disturbance of Type II cells might disrupt the restricted compartment, thereby enhancing measureable Ca^{2+} responses on depolarization. Following this idea, we applied relatively strong negative pressure (40–60 cm H2O) to 5 Type II cells and did indeed

observe increased Ca^{2+} responses in 3 of them (Fig.1H). These findings are consistent with the hypothesized special compartmentalization of CALHM channels and atypical mitochondria playing a role in restriction of Ca^{2+} influx.

Localization of CALHM1 Channels

In order to assess the relationship between the CALHM1 channels, mitochondria and purinoceptive nerve fibers, we undertook high resolution immunohistochemical examination of taste buds. Immunohistochemistry for CALHM1 using an antibody mapping to residues 318 to 328 on the intracellular domain of human CALHM1 (Suppl Fig. 1A) reveals small (1–2 μm) elongate patches of reactivity associated with the plasma membrane of Type II taste cells identified by expression of GFP driven by the promotor of the taste transduction channel TrpM5 (Fig. 2). Such patches are not seen in tissues prepared from CALHM1 knockout animals (Suppl Fig 1B). Further, triple label immunohistochemistry shows at the light microscopic level, a close relationship between these CALHM1 patches and zones of contact between the Type II cells and nerve fibers expressing the P2X2 purinergic receptors (Fig 2A–E). Such restriction of channels to a focal basolateral compartment is not noted for other taste transduction components of Type II taste cells including TrpM5 ((24)) and various Na-channels ((25)).

In order to assess whether CALHM1 channels were localized appropriately to serve as the release channels associated with atypical mitochondria, we used immunohistochemistry to compare the distribution of CALHM1 channels and mitochondria, identified with cytochrome C immunostaining (CytC). The clusters of CALHM1 localize to sites displaying patches of CytoC activity appropriate in size to be the atypical mitochondria (Fig. 3A–C). Taken together, these results suggest a close association between the CALHM1 channel and atypical mitochondria as well as between the CALHM1 channel and purinoceptive nerve fibers.

Ultrastructural localization of the CALHM1 channels shows specific localization of the channel to the membrane subjacent to the atypical mitochondria (Fig.3D–E) and always adjacent to a nerve fiber profile. No aggregates of CALHM1 label occur at other locations in the taste cells.

Relationship of ‘Atypical’ Mitochondria to CALHM1 and Nerve Fibers

We investigated the possibility that the CAHLM1 channels are specifically associated with previously described ‘atypical’ mitochondria and that both localize to points of contact between Type II cells and nerve fibers. To date, it has been unclear whether the atypical mitochondria occur only in Type II cells, and then only at taste-cell neurite contacts, or are distributed more widely. In many cells, mitochondria are polymorphic with different-appearing mitochondria situated at specific locations in a cell. For example, in photoreceptors, densely clustered mitochondria partition the cell into separate domains: cell body and outer segment (32). In that context, the mitochondria are crucial in maintaining distinct Ca^{2+} compartments in the two domains.

In order to test whether the atypical mitochondria in taste cells are specifically associated with neuronal contacts, we used ultra-resolution confocal microscopy (Fig. 2D–E) on

specimens stained for CALHM1 and P2X2 or P2X3 receptors. In addition we employed serial blockface scanning electron microscopy (sbfSEM) to reconstruct the relationships between taste cells and nerve fibers in 4 taste buds from the circumvallate papillae of 3 mice. As shown in Fig. 2, CAHLM1 immunoreactivity is localized to small spots along the surface of Type II taste cells, identified by the GFP label. At each of these CALHM1 spots, a P2X-immunoreactive nerve fiber is evidently in contact with the taste cell. In our sbfSEM samples, of the more than 125 atypical mitochondria identified, ranging in size from 0.5 – 3 μm in length, all but 1 lie at the point of contact between a Type II taste cell and an afferent nerve fiber (Fig. 4 and Suppl. Videos S1, S2). Individual taste cells often possess multiple atypical mitochondria at the contact points with a single adjacent nerve fiber (Fig. 4A′, B′, D, D′; Suppl. Videos S1, S2). Moreover, no conventional mitochondria lie closely apposed to the membrane of Type II taste cells at points of contact with nerve fibers, although we did identify 3 transitional mitochondria showing features of both atypical and conventional organization of cristae.

Reconstructions of all mitochondria in two of these cells shows that the atypical mitochondria are distinct organelles, essentially disconnected from the network of conventional mitochondria within the same cell (Fig. 4C; Supplementary Video S3). The relationship between the atypical mitochondrion, the taste cell plasma membrane and neurite membrane showed a rigid dimensionality (Fig. 5) with the estimated distance between mitochondria and taste cell plasma membrane being ~20–30 nm (Fig. 5) and a corresponding intercellular distance between nerve and taste cell (synaptic cleft) of ~10–15 nm. Based on 3D reconstructions (Fig. 5B) and analysis of mitochondrial sizes we estimated the volumes of these spaces for a medium-sized atypical mitochondrion (1.4 μm across and 2 μm long) to be about 0.04 – 0.08 fl.

Ultrastructure of ‘Atypical’ Mitochondria

The atypical mitochondria at taste cell-nerve fiber contacts possess unusually large tubular cristae in contrast to the thin parallel cristae of conventional mitochondria (Fig. 4E, F; 5A, Suppl. Video S4). The structure of cristae within mitochondria differs according to many factors including bioenergetic state and ATP synthase dimerization, lipid composition, and fission-fusion events (33). In mitochondria, ATP-synthase on the crista membranes generates ATP which is rapidly moved by ATP translocase from the mitochondrial matrix into the luminal space continuous with the intermembrane space between the outer mitochondrial membrane and the walls of the cristae. Once in the intermembrane space, the ATP leaves the mitochondrion through VDAC (porin) channels abundant in the outer membrane. Our measurements of conventional mitochondria (n= 18; Table 1) within the Type II taste cells show that the intermembrane space represents about 10–12% of the total volume of the mitochondrion, as it does in many other mitochondrial systems (9.8% – 20%) in the nervous system (34, 35). In contrast, the intermembrane volume of the atypical mitochondria (n = 20; Table 1) accounts for about 38% of the total mitochondrial volume (atypical = 0.38+/−0.005 s.d; typical = 0.11+/−0.003 s.d.; t-test, $p < 0.0001$). While ATP in intermembrane space should readily diffuse through the VDAC channels on the external bounding membrane of the mitochondrion, the large size of the atypical mitochondrion coupled with its larger intermembrane space may offer a relatively large reservoir of newly synthesized ATP

available to buffer local release. For a mid-sized atypical mitochondrion, we estimate the volume of the intermembrane space would be about 1.2 femtoliters, considerably larger than the 0.04–0.08 femtoliter volume of the restricted space between the atypical mitochondrion and the plasma membrane of the cell. Taken together with our data on the consistent spacing of the mitochondria and plasma membrane of the taste cell, these findings suggest the possibility of a unique presynaptic compartment that ensures robust and specific non-vesicular ATP storage and release onto nerve fibers via gated release channels. Also, the restricted space between the mitochondrial outer membrane and the plasma membrane of the taste cell coupled with the ability of mitochondria to take up free Ca^{2+} may account for the limited diffusion of Ca^{2+} into the taste cell upon opening of the CALHM1 channel(36).

Role of Mitochondria in ATP Release

Since Type II taste cells release ATP in response to depolarization, but lack synaptic vesicles, a likely source of ATP is the atypical mitochondria associated with the taste cell-nerve fiber contact. To test the necessity for active production of ATP in the release process, we used oligomycin, an inhibitor of ATP-synthase, to block production of ATP by oxidative phosphorylation in mitochondria but leaving intact the ability of the cell to generate ATP by direct glycolysis. Using ATP biosensors to monitor efflux of ATP from oligomycin-treated cells, we found that ATP efflux lasted 3–5 min, but declined rapidly thereafter (Fig. 6; Suppl Fig. 2), although the taste cells themselves as well as the biosensor cell remained physiologically functional in terms of being capable of generating Ca^{2+} responses to exogenous activators even in the presence of oligomycin (Suppl. Fig. 2). Furthermore, after depletion of the mitochondrial ATP store by oligomycin, the taste cells then release ADP (Fig. 6D), which likely originates from the accumulation of ADP in the intermembrane space of the mitochondria in the absence of ATP synthase activity and resulting cessation of translocase activity. These results indicate that taste cells release ATP produced in mitochondria and suggest the existence of a pool of releasable ATP that is poorly exchangeable with the bulk of cytosolic ATP. The ultrastructure of the atypical mitochondria and junctional relationships between the taste cell and the nerve fiber are consistent with this hypothesis. Assuming that the pool of ATP in the cytoplasm in the 0.04–0.08 fl space between the mitochondrion and the plasma membrane represents the readily releasable pool, then the 1.4 fl volume within the mitochondrial intermembrane space would represent the reservoir by which the releasable pool is refilled during and after channel opening.

Further implicating mitochondria in release of ATP by taste cells is the fact that carbenoxolone (CBX) inhibits this release, which previous studies had attributed to block of pannexin (Pnx1) channels then believed to be the route of release (16–18, 30). We now know that CALHM1, not Pnx1, is the crucial release channel, so why then should CBX interfere with ATP release? One possibility is that CBX can collapse the mitochondrial potential (37, 38), which would halt production of ATP thereby reducing ATP release. To test this, we loaded the mitochondrial potential dye (Mito-ID) into taste cells in controls and in the presence of CBX in preparations of non-dissociated taste buds. When Mito-ID dye was applied simultaneously with 10 μM CBX (sufficient to inhibit ATP secretion in taste cells) (17, 18), intra-mitochondrial orange fluorescence exhibited a bell-shaped distribution as a function of incubation time (Suppl. Fig 3) suggesting that CBX treatment substantially

reduced mitochondrial potential and consequently reduced ATP synthesis. Thus, the reduction in ATP release upon application of CBX should not be considered a reliable measure of channel activity but may be a measure of mitochondrial efficiency. Accordingly, our hypothesis of a mitochondrial origin of ATP and efflux via CALHM1 channels resolves the apparent inconsistency between the effects of CBX and the pharmacological profile of CALHM1 (see (39) for discussion).

Discussion

In this study, we show the existence of a novel synaptic signaling complex in Type II taste receptor cells formed by clustered ATP-permeable CALHM1 channels and atypical mitochondria apposed to points of contact with purinoceptive nerve endings. This ATP-release machinery is fast and strong enough to release detectable levels of ATP, the afferent taste neurotransmitter, into the intercellular space even in response to short-term taste stimulation accompanied by generation of several action potentials (18). Here, we provide experimental support for the idea that ATP-permeable CALHM1 channels are clustered and that the corresponding submembrane compartment is physically separated from the bulk of the cytoplasm by atypical mitochondria (Fig. 7). The unique organization of this compartment protects the cell from metabolite leakage through the large pore channel and allows for specific and precise non-vesicular, regulated neurotransmission.

CALHM1 is a nonselective channel permeable to many ionic species, with relative permeabilities following the sequence Ca:Na:K:Cl ~ 11:1:1.2:0.6 (40). Based on this permeability sequence, we estimate using the Goldman-Hodgkin-Katz current equations (41), a fractional current carried by Ca^{2+} ions to be nearly 30% at −50 mV but less than 1% at 50 mV. Such CALHM-1 or CALHM1-like currents have been recorded in taste buds from all three main taste fields in the tongue: circumvallate, foliate and fungiform papilla (16, 20, 42–44). As demonstrated recently, CALHM1 channels are largely responsible for large (~ 1 nA) inward tail currents in Type II cells (43), allowing one to estimate CALHM1-dependent conductance to be nearly 20 nS at 50 mV. With this steady-state conductance and for characteristic times of CALHM1 activation and deactivation at 50 mV of about 20 ms and 10 ms, respectively (22), action potentials should stimulate loading of about 10^6 Ca^{2+} ions. This would result in a rise in Ca^{2+} concentration by nearly 10 mM in the the 0.08 fl volume of the sub-mitochondrial compartment. That we observe only negligible or small Ca^{2+} signals generated due to activity of CALHM1 channels in Type II cells (Fig.3A), argues for the existence of a mechanism that provides limitation of influx and/or effective clearance of Ca^{2+}. Since the TrpM5 transduction channel of Type II taste cells is gated by intracellular Ca^{2+}, wholesale rises in intracellular Ca^{2+} would likely open TrpM5 channels thereby further depolarizing the taste cells. That such positive feedback does not occur suggests that Ca^{2+} influx and diffusion must be limited. In conventional synaptic terminals (45), Ca^{2+} is cleared both by mitochondrial uptake and plasma membrane Ca^{2+}-ATPase (PMCA). The large reservoir of ATP in the atypical mitochondrion of taste cells should offer a ready supply of ATP required to drive PMCA-mediated removal of Ca^{2+} as well as providing a local source of ATP for release.

The intimate relationship between the atypical mitochondrion and the CALHM1 channels offers an unconventional means for quantal-like release of ATP in the absence of synaptic vesicles. Each action potential in a Type II taste cell stimulates the release of a near-constant amount of neurotransmitter (16, 18) leading to a scaled system translating the magnitude of the taste cell response into a proportionate neural response. Because of the large intra-mitochondrial reservoir of ATP adjacent to the release channels, this process is likely independent of the short-term overall cellular metabolic status, including the activities of other energy-consuming intracellular processes. At the immunological synapse, mitochondria also are necessary for the production and release of ATP crucial for regulation of T-cell function (46).

Other axonless sensory cells, including rod and cone photoreceptors, hair cells, and even Type III taste cells, utilize classical chemical synapses to release neurotransmitters. In addition, photoreceptors also exhibit non-vesicular release of neurotransmitter via reversal of neurotransmitter transporters (47, 48). Release via these transporters is, however graded, i.e. not quantal, and occurs diffusely across widespread areas of cell membrane, rather than at a specialized synaptic focus. It is currently unclear why Type II cells adopt a specialized channel-based release system rather than the typical SNARE-based vesicular exocytotic mechanism used by other receptor cells. CALHM1-mediated release of ATP and its association with atypical mitochondria that we find in taste buds may be more common in other neuronal systems, yet not fully recognized. CALHM1 is expressed in hippocampal neurons and a polymorphism in this channel influences the onset of Alzheimer's disease and affects Ca^{2+} homeostasis(49). In neurons, CALHM1 plays an important role in Ca^{2+} homeostasis and flux through the membrane, especially in response to low extracellular Ca^{2+}(50). Whether CALHM1 in central neurons also forms clusters associated with specialized mitochondria to regulate release of ATP requires further investigation.

The situation of the atypical mitochondria only at points of contact with nerve fibers suggests the presence of signaling between the afferent fiber and the taste cell similar to the signal between antigen-presenting cells and T cells (2). In that immunological system, a key signal is the cell adhesion molecule, ICAM-1 along with other factors. Upon recognition of the signal, the cytoskeleton and mitochondria of the T-cell reorganize to form the specialized immunological synapse. In the taste system, it is likely that a cell surface molecule on the nerve fiber, e.g NCAM, may trigger the clustering of the CALHM1 channel and reorganization of the local mitochondria. The exact nature of the intercellular signals in the taste system and subsequent cascade of events leading to the development of the mitochondrial-CALHM1 synapse remain to be elucidated.

Materials & Methods

Animals

Mice were utilized in all experiments involving live animals. All experimental protocols were in accordance with local regulatory bodies: the European Communities Council Directive (86/609/EEC) and approved by the regional ethical committee (Stockholms Norra Djurförsöksetiska Nämnd; N512/12) and by the Animal Care Committee of the Institute of Cell Biophysics, Pushchino; or by the local Animal Care and Use Committees at the The

Feinstein Institute for Medical Research, North Shore LIJ Health System or at the Univ. Colorado School of Medicine. Particular effort was directed to minimize the number of animals and their suffering during the experiments.

Tissue preparation, immunohistochemistry and imaging

Wild-type and TrpM5-GFP (Tg(Trpm5-EGFP)$^{\#Sdmk}$) transgenic mice (to reveal Type II taste cells) were perfused with a fixative composed of 4% paraformaldehyde (PFA) and 0.05% glutaraldehyde in 0.1M phosphate buffer (PB, pH7.4) that was preceded by a short rinse with physiological saline (anesthesia: 5% isoflurane or Fatal-Plus Solution® [pentobarbital] Vortech Pharmaceuticals, Dearborn, MI,). After post-fixation in the same fixative 3 hr - overnight and cryoprotection in 10%–20% sucrose for 12 – 48h, tongues were cryo-sectioned at 12 – 20 μm thickness and dried onto positively-charged glass slides.

In some specimens, antigen retrieval was carried out either using Dako solution (Dako S1699) or 10mM sodium citrate (pH 9 for 10 minutes at 85°C) prior to exposure to antisera to enhance antigen accessibility. Other sections were exposed to antibodies without antigen retrieval. Sections were then exposed for 16 – 72h at 4 °C to select combinations of primary antibodies diluted in PB or PBS to which 0.1 – 2% normal donkey serum and 0.3% Triton X-100 had been added. After extensive rinsing in PB, antibodies were revealed by fluorescent secondary antibodies 2h at 22 – 24 °C: donkey anti-rabbit and anti-mouse (carbocyanine (Cy)2, 3 or 5-tagged at 1:200; Jackson Immuno Research Laboratories; West Grove, PA); donkey anti-mouse A568 (Life Technologies; Carlsbad, CA); goat anti-rabbit A649 or donkey anti-chicken A488 (Jackson) at 1:400 dilution each). After 3 additional washes, sections were coverslipped with glycerol-based solution or with Fluoromount G (Southern Biotechnology Associates, Birmingham, AL). Primary antibodies employed were: mouse monoclonal antibody 32C2 directed against the C-terminal domain of CALHM1 at 1:50 dilution (51); rabbit polyclonal antibody against cytochrome C (Santa Cruz, sc-7159; AB_2090474); rabbit anti-P2X3 at 1:1000 dilution (APR-016; Alomone Labs; Jerusalem, Israel; AB_2341047); chicken anti GFP at 1:1000 dilution (Aves Labs; Tigard, OR; AB_10000240). All staining reported herein was absent when the primary antibody was omitted.

For ultrastructural immunohistochemistry, tissues were fixed as above, and then sectioned on a vibratome at 80μm and collected in phosphate buffer. Sections containing taste buds were incubated with 1% $NaBH_4$ for 10 minutes, rinsed and then transferred to 10 mM sodium citrate (pH 6) and 0.05% Tween 20 for 10 min at 85 °C. Afterwards, sections were placed for 15 mins. into an avidin-biotin blocking system involving exposure of the tissue first to Avidin D followed by incubation in unlabeled biotin (Vector SP-2001) containing 2% normal donkey serum plus AB media, then exposed to unlabeled goat anti mouse IgG Fab (1:25, Cat. 115-007-003, Jackson ImmunoResearch) for 1 hour to block non-specific binding of secondary antisera to endogenous IgG. The sections then were incubated with primary antibody monoclonal CALHM1 (1:20) for 4 nights. After washing, the sections were incubated overnight to biotinylated rat anti mouse IgG2a (1:1000, Cat. 04-6240, Life Technologies), then incubated with ABC (Vector Laboratories, Burlingame, CA) for two hours. The sections were treated for 10 min in 0.05 M Tris Buffer (pH 7.3) containing 0.05%

DAB. The label was visualized by floating the sections for 2–4 min in the fresh DAB mixture with hydrogen peroxide (0.002%).

Images were acquired on either an Olympus Fluoview Confocal microscope or on Zeiss LSM 700, LSM 710 or LSM 780 confocal laser-scanning microscopes with maximal signal separation or spectral scanning. Some images of Fig. 2 were processed with Zeiss Airyscan™. Composite figures were assembled in CorelDraw X5 or Photoshop CC 2014 (Adobe).

32C2 antibody specificity assessment by epitope blocking

Peptide array for epitope mapping was employed to determine the exact epitope sequence of the mouse IgG2a monoclonal antibody (32C2) against CALHM1. Ten-residue-long peptides, with an offset of 3 residues covering the entire cytosolic C-terminal end of human CALHM1, were dotted on nitrocellulose membrane. The membrane was then processed for Western Blot using 32C2, as previously described (51). The identified epitope peptide was used for antibody blocking. HT-22 cells were transiently transfected with empty vector or human CALHM1. Protein extracts were then processed by SDS-PAGE and transferred on nitrocellulose membranes. 32C2, pre-incubated 1h at room temperature with the indicated peptides (0.2 μg/mL) in 5% milk tween-TBS, was then used for WB.

Serial Blockface Scanning EM (sbfSEM) and Transmission electron microscopy

Methods for 3D-EM imaging and volumetric analysis are slightly modified from those described previously (52, 53). Mice were anesthetized with Fatal-Plus Solution® and perfused with 0.1% $NaNO_2$, 0.9% NaCl, and 200 units sodium heparin in 100 ml 0.1 M phosphate buffer pH7.3, at 35°C followed by 2.5% glutaraldehyde and 2% formaldehyde with 2mM $CaCl_2$ in 0.025 M cacodylate buffer pH7.3 at 35° C for 10 minutes. Tissues are removed and placed in the same fixative for 2–3 hours on ice, then cut into 200 μm thick vibratome sections.

For conventional transmission EM, some thick sections prepared as for sbfSEM, were rinsed in buffer, then stained with 2% osmium tetrooxide in 0.05 M Sodium Cacodylate Buffer for 30 min. After rinsing, the sections were placed overnight in 1% uranyl acetate in double-distilled H_2O and then stained en bloc in Walton's lead at 60°C for 40 min prior to embedment in Luft's Epon. Thin sections (90–120 nm) were cut with a diamond knife on a Reichert Ultracut E ultramicrotome, examined with FEI Tecnai G2 Biotwin Transmission Electron Microscope, photographed with Gatan Ultrascan 1000 digital camera.

Vibratome sections (200 microns thickness) for sbfSEM were rinsed with 0.025 M cacodylate buffer pH7.3 containing 2mM $CaCl_2$, then incubated for 1 hour at 0°C in a solution containing 3% K4[Fe(CN)6] in 0.025M cacodylate buffer pH7.3 with 2mM $CaCl_2$ combined with an equal volume of 4% aqueous OsO_4. After the first heavy metal incubation, the sections are washed with H_2O at room temperature 5×3 min. then placed in 1% thiocarbodydrazide solution for 20 min at room temperature. After washing, the sections are placed in 2% OsO_4 for 30 min at room temperature. Following this second exposure to osmium, the tissues are washed in H_2O 5×3 min at room temperature, then placed in 1% ($UO_2(CH_3COO)_2$·2H2O) and left in a refrigerator overnight. The next day, en bloc Walton's

lead aspartate staining is performed for 30 min at 60°C in 0.066 g of $Pb(NO_3)_2$ in 10 ml of aspartic acid stock and pH adjusted to 5.5 with 1N KOH. Sections are dehydrated using an increasing series of ice-cold alcohol solutions before transfer into propylene oxide 5×3 min. and final embedment in Lufts Epon 3:7 at 60°C overnight.

The tissues are then trimmed and mounted on an aluminium pin, coated with colloidal silver paste around the block edges, and then examined in a Zeiss Sigma VP system equipped with a Gatan 3View in-chamber ultramicrotome stage with low-kV backscattered electron detectors optimized for 3View systems. Samples are routinely imaged at 2.25kV, at 5–10nm/pixel resolution (30μm aperture, high current mode, high vacuum), with field sizes between 80–250 μm in x,y and approximately 500 slices with 80 nm thickness were generated. The resulting image stacks are aligned and montaged in Photoshop® (Adobe Systems) and ImageJ. Segmentation and reconstruction is accomplished using *Reconstruct* software.

Measurement of Mitochondrial Intermembrane Space

Atypical and typical mitochondria were selected from virtual sections derived from sbfSEM image stacks as viewed in Reconstruct. These mitochondrial types were distinguished based on several morphological features including overall size of the mitochondrion and exaggerated tubular shape of the cristae. Images were imported into Amira 5.6.0 (FEI Company, Hillsboro, Oregon) for volumetric analysis.

A total of 20 atypical mitochondria and 18 typical mitochondria from a total of 3 different taste buds were analyzed. Typical mitochondria were selected to match approximately in terms of overall profile area of the atypical mitochondria measured. Either 3 or 4 profiles were analyzed per mitochondrion according to total number of profiles through the particular mitochondrion.

Using the “MaterialStatistics” measurement function, we measured the total area of each mitochondrial profile as well as the area of the intermembrane space including the area within the tubular cristae. We then calculated the ratio of intermembrane space to total mitochondrial area for each mitochondrial profile. Within each class of mitochondrion, typical and atypical, no significant differences existed between samples or for different mitochondrial sizes. Accordingly data from the different sizes of mitochondria were pooled for a statistical comparison using an unpaired t-test on Graphpad (www.graphpad.com/quickcalcs)..

Taste cell isolation

For isolation of taste buds or individual cells, 8–10 weeks old C57Bl6 mice were euthanized with CO_2 followed by cervical dislocation before tongues were removed. Taste cells were isolated from mouse (NMRI, 6–8-week old) circumvallate (CV) papilla. A tongue was injected between the epithelial and muscle layers with 0.7 mg/ml collagenase B, 1 mg/ml dispase II, 0.2 mg/ml elastase (all from Roche Diagnostics), and 0.5 mg/ml trypsin inhibitor (Sigma-Aldrich) dissolved in a solution (mM): 140 NaCl, 20 KCl, 0.3 $MgCl_2$, 0.3 $CaCl_2$, 10 HEPES-NaOH (pH 7.4). The tongue was incubated in an oxygenated Ca-free solution (in mM): 120 NaCl, 20 KCl, 1 $MgCl_2$, 0.5 EGTA, 0.5 EDTA, 10 HEPES-NaOH (pH 7.4) for 20–30 min. The epithelium was then peeled off from the underlying muscle, pinned serosal

side up in a dish covered with Sylgard resin, and incubated in the Ca-free solution for 10–30 min. The isolated epithelium was kept at room temperature in a solution (mM): 130 NaCl, 10 $NaHCO_3$, 5 KCl, 1 $MgCl_2$, 1 $CaCl_2$, 10 HEPES-NaOH (pH 7.4), 5 glucose, 2 Na-pyruvate). Taste cells were removed from the CV papilla by gentle suction with a firepolished pipette with an opening of 70–90 μm and then expelled into an electrophysiological chamber.

ATP and ATP/ADP biosensors and Calcium imaging

Cells of the COS-1 line that endogenously express P2Y receptors coupled to Ca^{2+} mobilization and CHO, were transfected with P2X2/P2X3 expression construct and used as cellular sensors for monitoring ambient nanomolar ATP and ADP concentrations. The bath solution for cellular physiology experiments contained (mM) 140 NaCl, 2.5 KCl, 1 $MgSO_4$, 1.3 $CaCl_2$, 1.2 NaH_2PO_4, 10 glucose, 5 pyruvate, 10 HEPES–NaOH, pH 7.4. For calcium imaging ATP-sensitive cells were preloaded with 4 mM Fluo-4AM+1.5 mg/ml Pluronic (both from Molecular Probes) for 30 min at 23–25°C. Cell fluorescence was excited with a computer controlled light emitting diode (Luxion) at 480 nm and recorded at 535 nm. Sequential fluorescence images were acquired every 0.5–2 seconds using a fluorescent Axioscope-2 microscope, an EMCCD Andor iXON camera (Andor Technology) and Workbench 6.0 software (INDEC Biosystems).

Cells were stimulated by bath application of compounds. All chemicals were from Sigma-Aldrich. Experiments were carried out at 23–25°C.

Electrophysiology and calcium imaging

Taste cells were assayed with the patch-clamp technique using the perforated patch (with 400 mg/l amphotericin B in the recording pipette) or whole-cell configuration. Ion currents were recorded, filtered, and analyzed using an Axopatch 200B amplifier, a DigiData1322 interface, and the pClamp8 software (Axon Instruments). Intracellular solution contained (mM) 100 CsCl, 40 KCl, 1 MgATP, 1 EGTA, 10 HEPES–NaOH, pH 7.4. The bath solution contained (mM) 140 NaCl, 2.5 KCl, 1 $MgSO_4$, 1.3 $CaCl_2$, 1.2 NaH_2PO_4, 10 glucose, 5 pyruvate, 10 HEPES–NaOH, pH 7.4.

For calcium imaging cells were loaded with 4 μM Fluo-4AM or FURA-2AM +1.5 mg/ml Pluronic (both from Molecular Probes) for 30 min at 23–25°C. For Fluo-4 loaded cells fluorescence was excited with a computer controlled light emitting diode (Luxion) at 480 nm and recorded at 535 nm. Sequential fluorescence images were acquired every 0.5–2 seconds using a fluorescent Axioscope-2 microscope, an EMCCD Andor iXON camera (Andor Technology) and Workbench 6.0 software (INDEC Biosystems). To measure Fura-2 signals, recordings were done using a VisiChrome monochromator and VisiView software (Visitron Systems) on an AxioExaminer.D1 microscope (Zeiss) equipped with a CoolSnap HQ^2 camera (Photometrics). Cells were stimulated by bath application of compounds. All chemicals were from Sigma-Aldrich. Experiments were carried out at 23–25°C.

Statistical analysis

Physiological data were analyzed using SigmaPlot (Systat Software Inc.). Data were expressed as means ± s.e.m. A p value of < 0.05 was considered statistically significant, and calculated by Student's t-test or Mann-Whitney rank sum test.

Supplementary Material

Refer to Web version on PubMed Central for supplementary material.

Acknowledgments

The authors thank Nicole Shultz and Mei Li for assistance with immunohistochemistry; Rae Russell and Remy K. Johnson for segmentations and reconstructions from serial blockface SEM data, and Samantha Fore (Carl Zeiss Microscopy, LLC) for assistance in acquiring the Airyscan images. We also appreciate the following for review of this manuscript at various stages in its preparation and finalization: Farrukh Abbas Chaudhry, University of Oslo, Oslo, Norway; Kurt Beam and Sue C. Kinnamon, Univ. Colorado Sch. Medicine; Emily Liman, Univ. Southern California.

Funding: S.S.K. was supported by Russian Academy of Sciences (Program #7) and Russian Foundation for Basic Research (grant 13-04-40082). I.A. was supported by Swedish Research Council, Bertil Hallsten Research Foundation, Jeassons Foundation, Strategic Regeneration Foundation and Knut and Alice Wallenberg Foundation (CLICK). T.H. was funded by the Swedish Research Council, Swedish Brain Foundation, Novo Nordisk Foundation, Petrus and Augusta Hedlunds Foundation, ERC Advanced Grant ("Secret-Cells", ERC-AdG-2015-695136), and the European Commission Integrated Project "PAINCAGE". R.A.R. was an EMBO long-term research fellow (ALTF 596-2014) co-funded by the European Commission FP7 (Marie Curie Actions, EMBOCOFUND2012, GA-2012-600394). R.A.R. is also supported by Ministry of Education and Science of the Russian Federation (Agreement no 14.575.21.0074 with Immanuel Kant Baltic Federal University, project leader – V.Kasymov). T.E.F. R.S.L., B.H., R.Y., G.J.K. and J.C.K. are supported by grants from the National Institute for Deafness and Communicative Disorders of the National Institutes of Health (U.S.A.), Grants 1R21DC013186 and R01DC014728 to T.E.F. and P30DC004657 to D. Restrepo (Univ. Colorado Sch. Medicine). P.M. was supported by a grant from the National Institute on Aging of the National Institutes of Health (R01AG042508).

References

1. Foster, M., Sherrington, SC. A Textbook of Physiology, Part 3. 7. Macmillan; London: 1897.
2. Grakoui A, Bromley SK, Sumen C, Davis MM, Shaw AS, Allen PM, Dustin ML. The immunological synapse: a molecular machine controlling T cell activation. Science. 1999; 285:221. published online EpubJul 09. [PubMed: 10398592]
3. Finger TE, Danilova V, Barrows J, Bartel DL, Vigers AJ, Stone L, Hellekant G, Kinnamon SC. ATP signaling is crucial for communication from taste buds to gustatory nerves. Science. 2005; 310:1495. published online EpubDec 2. doi: 10.1126/science.1118435 [PubMed: 16322458]
4. Vandenbeuch A, Larson ED, Anderson CB, Smith SA, Ford AP, Finger TE, Kinnamon SC. Postsynaptic P2X3-containing receptors in gustatory nerve fibres mediate responses to all taste qualities in mice. J Physiol. 2015; 593:1113. published online EpubMar 1. doi: 10.1113/jphysiol.2014.281014 [PubMed: 25524179]
5. Vandenbeuch A, Anderson CB, Ford AP, Smith S, Finger TE, Kinnamon SC. A selective P2X3, P2X2/3 receptor antagonist abolishes responses to all taste stimuli in mice. Chem Senses. 2013; 38:86.doi: 10.1093/chemse/bjt036)
6. Bo X, Alavi A, Xiang Z, Oglesby I, Ford A, Burnstock G. Localization of ATP-gated P2X2 and P2X3 receptor immunoreactive nerves in rat taste buds. Neuroreport. 1999; 10:1107. published online EpubApr 6. [PubMed: 10321492]
7. Yang R, Montoya A, Bond A, Walton J, Kinnamon JC. Immunocytochemical analysis of P2X2 in rat circumvallate taste buds. BMC Neurosci. 2012; 13:51.doi: 10.1186/1471-2202-13-51 [PubMed: 22621423]
8. Ishida Y, Ugawa S, Ueda T, Yamada T, Shibata Y, Hondoh A, Inoue K, Yu Y, Shimada S. P2X(2)- and P2X(3)-positive fibers in fungiform papillae originate from the chorda tympani but not the

trigeminal nerve in rats and mice. J Comp Neurol. 2009; 514:131. published online EpubMay 10. doi: 10.1002/cne.22000 [PubMed: 19266560]

9. Chaudhari N, Roper SD. The cell biology of taste. J Cell Biol. 2010; 190:285. published online EpubAug 9. doi: 10.1083/jcb.201003144 [PubMed: 20696704]
10. Huang AL, Chen X, Hoon MA, Chandrashekar J, Guo W, Trankner D, Ryba NJ, Zuker CS. The cells and logic for mammalian sour taste detection. Nature. 2006; 442:934. published online EpubAug 24 (nature05084 [pii]). doi: 10.1038/nature05084 [PubMed: 16929298]
11. Huang YA, Maruyama Y, Stimac R, Roper SD. Presynaptic (Type III) cells in mouse taste buds sense sour (acid) taste. J Physiol. 2008; 586:2903. published online EpubJun 15. doi: 10.1113/jphysiol.2008.151233 [PubMed: 18420705]
12. Clapp TR, Medler KF, Damak S, Margolskee RF, Kinnamon SC. Mouse taste cells with G protein-coupled taste receptors lack voltage-gated calcium channels and SNAP-25. BMC Biol. 2006; 4:7.doi: 10.1186/1741-7007-4-7 [PubMed: 16573824]
13. Medler KF, Margolskee RF, Kinnamon SC. Electrophysiological characterization of voltage-gated currents in defined taste cell types of mice. J Neurosci. 2003; 23:2608. published online EpubApr 1. [PubMed: 12684446]
14. Yang R, Crowley HH, Rock ME, Kinnamon JC. Taste cells with synapses in rat circumvallate papillae display SNAP-25-like immunoreactivity. J Comp Neurol. 2000; 424:205. published online EpubAug 21. [PubMed: 10906698]
15. Yang R, Tabata S, Crowley HH, Margolskee RF, Kinnamon JC. Ultrastructural localization of gustducin immunoreactivity in microvilli of type II taste cells in the rat. J Comp Neurol. 2000; 425:139. published online EpubSep 11. doi: 10.1002/1096-9861(20000911)425:1<139::AID-CNE12>3.0.CO;2-# [PubMed: 10940948]
16. Romanov RA, Rogachevskaja OA, Bystrova MF, Jiang P, Margolskee RF, Kolesnikov SS. Afferent neurotransmission mediated by hemichannels in mammalian taste cells. EMBO J. 2007; 26:657. published online EpubFeb 7. doi: 10.1038/sj.emboj.7601526 [PubMed: 17235286]
17. Huang YJ, Maruyama Y, Dvoryanchikov G, Pereira E, Chaudhari N, Roper SD. The role of pannexin 1 hemichannels in ATP release and cell-cell communication in mouse taste buds. Proc Natl Acad Sci U S A. 2007; 104:6436. published online EpubApr 10. doi: 10.1073/pnas.0611280104 [PubMed: 17389364]
18. Murata Y, Yasuo T, Yoshida R, Obata K, Yanagawa Y, Margolskee RF, Ninomiya Y. Action potential-enhanced ATP release from taste cells through hemichannels. J Neurophysiol. 2010; 104:896. published online EpubAug. doi: 10.1152/jn.00414.2010 [PubMed: 20519578]
19. Taruno A, Matsumoto I, Ma Z, Marambaud P, Foskett JK. How do taste cells lacking synapses mediate neurotransmission? CALHM1, a voltage-gated ATP channel. Bioessays. 2013; 35:1111. published online EpubDec. doi: 10.1002/bies.201300077 [PubMed: 24105910]
20. Taruno A, Vingtdeux V, Ohmoto M, Ma Z, Dvoryanchikov G, Li A, Adrien L, Zhao H, Leung S, Abernethy M, Koppel J, Davies P, Civan MM, Chaudhari N, Matsumoto I, Hellekant G, Tordoff MG, Marambaud P, Foskett JK. CALHM1 ion channel mediates purinergic neurotransmission of sweet, bitter and umami tastes. Nature. 2013; 495:223. published online EpubMar 14. doi: 10.1038/nature11906 [PubMed: 23467090]
21. Romanov RA, Bystrova MF, Rogachevskaya OA, Sadovnikov VB, Shestopalov VI, Kolesnikov SS. The ATP permeability of pannexin 1 channels in a heterologous system and in mammalian taste cells is dispensable. Journal of cell science. 2012; 125:5514. published online EpubNov 15. doi: 10.1242/jcs.111062 [PubMed: 22956545]
22. Romanov RA, Rogachevskaja OA, Khokhlov AA, Kolesnikov SS. Voltage dependence of ATP secretion in mammalian taste cells. J Gen Physiol. 2008; 132:731. published online EpubDec. doi: 10.1085/jgp.200810108 [PubMed: 19029378]
23. Corriden R, Insel PA. Basal release of ATP: an autocrine-paracrine mechanism for cell regulation. Sci Signal. 2010; 3:re1.doi: 10.1126/scisignal.3104re1 [PubMed: 20068232]
24. Kusumakshi S, Voigt A, Hubner S, Hermans-Borgmeyer I, Ortalli A, Pyrski M, Dorr J, Zufall F, Flockerzi V, Meyerhof W, Montmayeur JP, Boehm U. A Binary Genetic Approach to Characterize TRPM5 Cells in Mice. Chem Senses. 2015; 40:413. published online EpubJul. doi: 10.1093/chemse/bjv023 [PubMed: 25940069]

25. Gao N, Lu M, Echeverri F, Laita B, Kalabat D, Williams ME, Hevezi P, Zlotnik A, Moyer BD. Voltage-gated sodium channels in taste bud cells. BMC Neurosci. 2009; 10:20. published online EpubMar 12. doi: 10.1186/1471-2202-10-20 [PubMed: 19284629]
26. Royer SM, Kinnamon JC. Ultrastructure of mouse foliate taste buds: synaptic and nonsynaptic interactions between taste cells and nerve fibers. J Comp Neurol. 1988; 270:11. [PubMed: 3372732]
27. Roberts CD, Dvoryanchikov G, Roper SD, Chaudhari N. Interaction between the second messengers cAMP and Ca2+ in mouse presynaptic taste cells. J Physiol. 2009; 587:1657. published online EpubApr 15 (jphysiol.2009.170555 [pii]). doi: 10.1113/jphysiol.2009.170555 [PubMed: 19221121]
28. Bystrova MF, Romanov RA, Rogachevskaja OA, Churbanov GD, Kolesnikov SS. Functional expression of the extracellular-Ca2+-sensing receptor in mouse taste cells. Journal of cell science. 2010; 123:972. published online EpubMar 15. doi: 10.1242/jcs.061879 [PubMed: 20179105]
29. Trexler EB, Bukauskas FF, Bennett MV, Bargiello TA, Verselis VK. Rapid and direct effects of pH on connexins revealed by the connexin46 hemichannel preparation. J Gen Physiol. 1999; 113:721. published online EpubMay. [PubMed: 10228184]
30. Bao L, Samuels S, Locovei S, Macagno ER, Muller KJ, Dahl G. Innexins form two types of channels. FEBS Lett. 2007; 581:5703. published online EpubDec 11. doi: 10.1016/j.febslet.2007.11.030 [PubMed: 18035059]
31. Dahl G, Muller KJ. Innexin and pannexin channels and their signaling. FEBS Lett. 2014; 588:1396. published online EpubApr 17. doi: 10.1016/j.febslet.2014.03.007 [PubMed: 24632288]
32. Giarmarco MM, Cleghorn WM, Sloat SR, Hurley JB, Brockerhoff SE. Mitochondria Maintain Distinct Ca2+ Pools in Cone Photoreceptors. J Neurosci. 2017; 37:2061. published online EpubFeb 22. doi: 10.1523/JNEUROSCI.2689-16.2017 [PubMed: 28115482]
33. Mannella CA. Structure and dynamics of the mitochondrial inner membrane cristae. Biochim Biophys Acta. 2006; 1763:542. published online EpubMay–Jun. doi: 10.1016/j.bbamcr.2006.04.006 [PubMed: 16730811]
34. Perkins GA, Ellisman MH, Fox DA. Three-dimensional analysis of mouse rod and cone mitochondrial cristae architecture: bioenergetic and functional implications. Molecular vision. 2003; 9:60. [PubMed: 12632036]
35. Perkins GA, Renken CW, Frey TG, Ellisman MH. Membrane architecture of mitochondria in neurons of the central nervous system. J Neurosci Res. 2001; 66:857. [PubMed: 11746412]
36. Rizzuto R, De Stefani D, Raffaello A, Mammucari C. Mitochondria as sensors and regulators of calcium signalling. Nature reviews Molecular cell biology. 2012; 13:566. published online EpubSep. doi: 10.1038/nrm3412 [PubMed: 22850819]
37. Salvi M, Fiore C, Battaglia V, Palermo M, Armanini D, Toninello A. Carbenoxolone induces oxidative stress in liver mitochondria, which is responsible for transition pore opening. Endocrinology. 2005; 146:2306. published online EpubMay. doi: 10.1210/en.2004-1128 [PubMed: 15677764]
38. Azarashvili T, Baburina Y, Grachev D, Krestinina O, Evtodienko Y, Stricker R, Reiser G. Calcium-induced permeability transition in rat brain mitochondria is promoted by carbenoxolone through targeting connexin43. Am J Physiol Cell Physiol. 2011; 300:C707. published online EpubMar. doi: 10.1152/ajpcell.00061.2010 [PubMed: 21148408]
39. Kinnamon SC, Finger TE. A taste for ATP: neurotransmission in taste buds. Frontiers in cellular neuroscience. 2013; 7:264.doi: 10.3389/fncel.2013.00264 [PubMed: 24385952]
40. Ma Z, Siebert AP, Cheung KH, Lee RJ, Johnson B, Cohen AS, Vingtdeux V, Marambaud P, Foskett JK. Calcium homeostasis modulator 1 (CALHM1) is the pore-forming subunit of an ion channel that mediates extracellular Ca2+ regulation of neuronal excitability. Proc Natl Acad Sci U S A. 2012; 109:E1963. published online EpubJul 10. doi: 10.1073/pnas.1204023109 [PubMed: 22711817]
41. Hodgkin AL. The ionic basis of electrical activity in nerve and muscle. Biol Res. 1951; 26:339.
42. Romanov RA, Kolesnikov SS. Electrophysiologically identified subpopulations of taste bud cells. Neurosci Lett. 2006; 395:249. published online EpubMar 13. doi: 10.1016/j.neulet.2005.10.085 [PubMed: 16309836]

43. Ma Z, Saung WT, Foskett JK. Action Potentials and Ion Conductances in Wild-type and CALHM1-knockout Type II Taste Cells. J Neurophysiol. 2017; jn 00835 2016. published online EpubFeb 15. doi: 10.1152/jn.00835.2016
44. Bigiani A. Calcium Homeostasis Modulator 1-Like Currents in Rat Fungiform Taste Cells Expressing Amiloride-Sensitive Sodium Currents. Chem Senses. 2017; 42:343. published online EpubMay 01. doi: 10.1093/chemse/bjx013 [PubMed: 28334404]
45. Shutov LP, Kim MS, Houlihan PR, Medvedeva YV, Usachev YM. Mitochondria and plasma membrane Ca2+-ATPase control presynaptic Ca2+ clearance in capsaicin-sensitive rat sensory neurons. J Physiol. 2013; 591:2443. published online EpubMay 15. doi: 10.1113/jphysiol.2012.249219 [PubMed: 23381900]
46. Ledderose C, Bao Y, Lidicky M, Zipperle J, Li L, Strasser K, Shapiro NI, Junger WG. Mitochondria are gate-keepers of T cell function by producing the ATP that drives purinergic signaling. J Biol Chem. 2014; 289:25936. published online EpubSep 12. doi: 10.1074/jbc.M114.575308 [PubMed: 25070895]
47. Schwartz EA. Depolarization without calcium can release gamma-aminobutyric acid from a retinal neuron. Science. 1987; 238:350. published online EpubOct 16 (. [PubMed: 2443977]
48. Richerson GB, Wu Y. Dynamic Equilibrium of Neurotransmitter Transporters: Not Just for Reuptake Anymore. Journal of Neurophysiology. 2003; 90:1363. published online Epub2003-09-01 00:00:00. doi: 10.1152/jn.00317.2003 [PubMed: 12966170]
49. Dreses-Werringloer U, Lambert JC, Vingtdeux V, Zhao H, Vais H, Siebert A, Jain A, Koppel J, Rovelet-Lecrux A, Hannequin D, Pasquier F, Galimberti D, Scarpini E, Mann D, Lendon C, Campion D, Amouyel P, Davies P, Foskett JK, Campagne F, Marambaud P. A polymorphism in CALHM1 influences Ca2+ homeostasis, Abeta levels, and Alzheimer's disease risk. Cell. 2008; 133:1149. published online EpubJun 27. doi: 10.1016/j.cell.2008.05.048 [PubMed: 18585350]
50. Vingtdeux V, Chang EH, Frattini SA, Zhao H, Chandakkar P, Adrien L, Strohl JJ, Gibson EL, Ohmoto M, Matsumoto I, Huerta PT, Marambaud P. CALHM1 deficiency impairs cerebral neuron activity and memory flexibility in mice. Scientific reports. 2016; 6:24250. published online EpubApr 12. doi: 10.1038/srep24250 [PubMed: 27066908]
51. Dreses-Werringloer U, Vingtdeux V, Zhao H, Chandakkar P, Davies P, Marambaud P. CALHM1 controls the Ca(2)(+)-dependent MEK, ERK, RSK and MSK signaling cascade in neurons. Journal of cell science. 2013; 126:1199. published online EpubMar 01. doi: 10.1242/jcs.117135 [PubMed: 23345406]
52. Ohno N, Kidd GJ, Mahad D, Kiryu-Seo S, Avishai A, Komuro H, Trapp BD. Myelination and axonal electrical activity modulate the distribution and motility of mitochondria at CNS nodes of Ranvier. J Neurosci. 2011; 31:7249. published online EpubMay 18 (31/20/7249 [pii]. doi: 10.1523/JNEUROSCI.0095-11.2011 [PubMed: 21593309]
53. Deerinck T, Bushong E, Lev-Ram V, Shu X, Tsien R, Ellisman M. Enhancing serial block-face scanning electron microscopy to enable high resolution 3-D nanohistology of cells and tissues. Microscopy and Microanalysis. 2010; 16:1138.

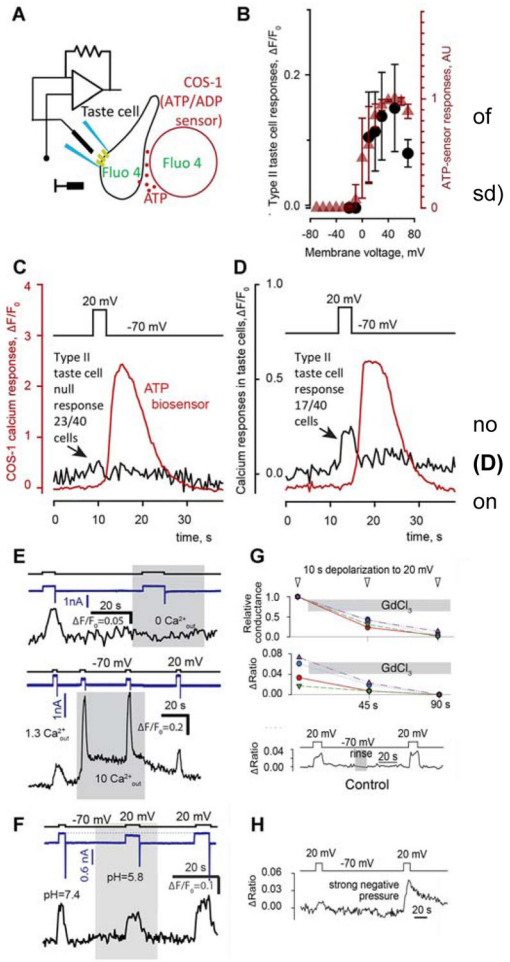

Fig. 1.

Depolarization-evoked Ca^{2+} signals in type II taste cells. (**A**) Preparation for simultaneous monitoring of intracellular Ca^{2+} and ATP release. (**B**) Calcium responses (black dots: mean ± sd) in taste cells showing a calcium response depend on the command voltage. Red triangles show voltage-dependence of the ATP release (data from Romanov et al (22)). **(C & D)**: Representative recordings showing: **(C)** no change in intracellular Ca^{2+} (n=23), and **(D)** small voltage-related Ca^{2+} signals (n=17) on depolarization. Black arrows indicate Ca^{2+} response while the red line shows ATP. (**E**) Changes in extracellular calcium leads to changes in Ca^{2+} responses. **(F)** Lowering extracellular pH leads to partial inhibition of currents and decrease of Ca^{2+}responses. (**G**) Application of extracellular 100 μM Gd^{3+} (gray bar) leads to decreases in current and Ca^{2+} responses (n=4), while no rundown occurs in the same time range in control preparations (bottom trace). (**H**) Negative pressure applied through the patch pipette increases calcium events in 3 of 5 cells.

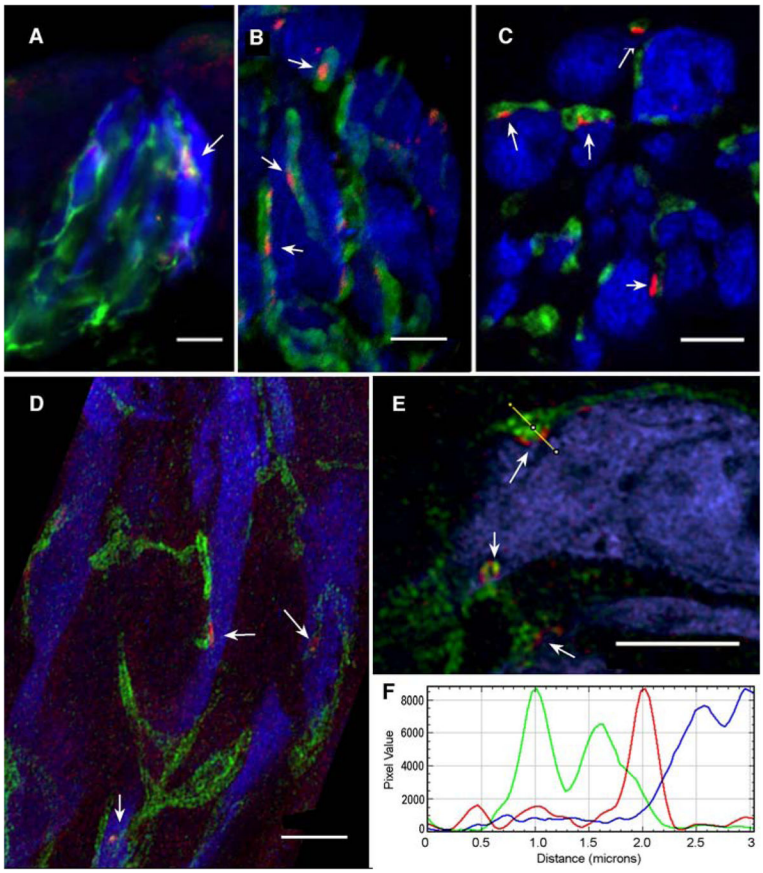

Fig. 2. CALHM1 lies at points of contact between taste cells and nerve fibers

(**A–E**) Immunostaining for CALHM1 (red), nerve fibers (P2X2 Green) and Type II taste cells (TrpM5- driven GFP, rendered in Blue). Punctate patches of CALHM1 (arrows) occur only in Type II taste cells and only at points of apposition with nerve fibers. Scale bars **A.** 10 μm; **B – E. 5** μm. **D.** Zeiss Airyscan image; others conventional LSCM. (**F**) A line plot of one such point of contact shown in panel E shows that the CALHM1 staining (red curve) lies between the Type II cell cytoplasm (blue curve) and the nerve membranes (bimodal green line).

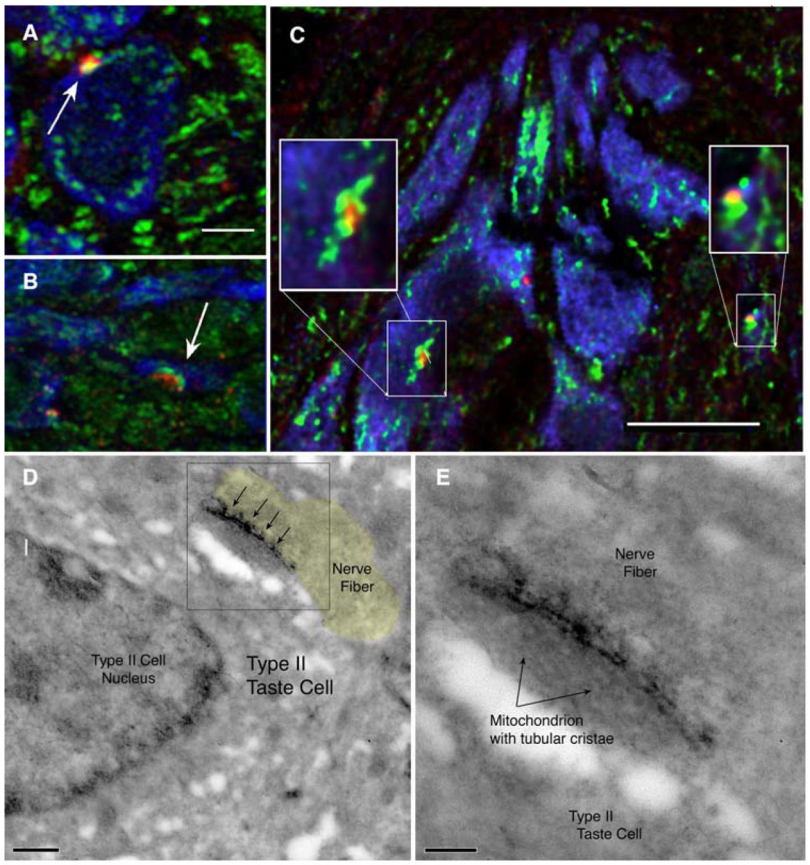

Fig. 3. CALHM1 lies adjacent to large mitochondria

(A–C) Colocalization of CALHM1 (red) and Cytochrome C (green) marking mitochondria. The CALHM1 patches (arrows) are always associated with one or more large mitochondria. Type II taste cells (TrpM5- driven GFP) rendered in Blue. Scale bar in A & B = 2 μm. Scale bar in C is 10μm with insets at 2x digital magnification and Unsharp Mask of 7.5 pixels at 85%. See Supplementary Fig. 4 for validation of the CALHM1 antibody. **D & E**. Electron micrographs of a taste cell-neurite contact immunoreacted for CALHM1 with peroxidase-based detection system. The dark immunoreaction product (arrows) lies at the interface between the taste cell membrane and the atypical mitochondrion consistent with the intracellular location of the CALHM1 epitope recognized by the antibody. Panel **E** is an enlargement of the boxed area in Panel **D.** Scale bar in **D** is 500nm; in **E** the scale bar is 200nm. The nerve fiber process is shaded yellow in panel **D** to facilitate visualization of the different structures in this unstained section.

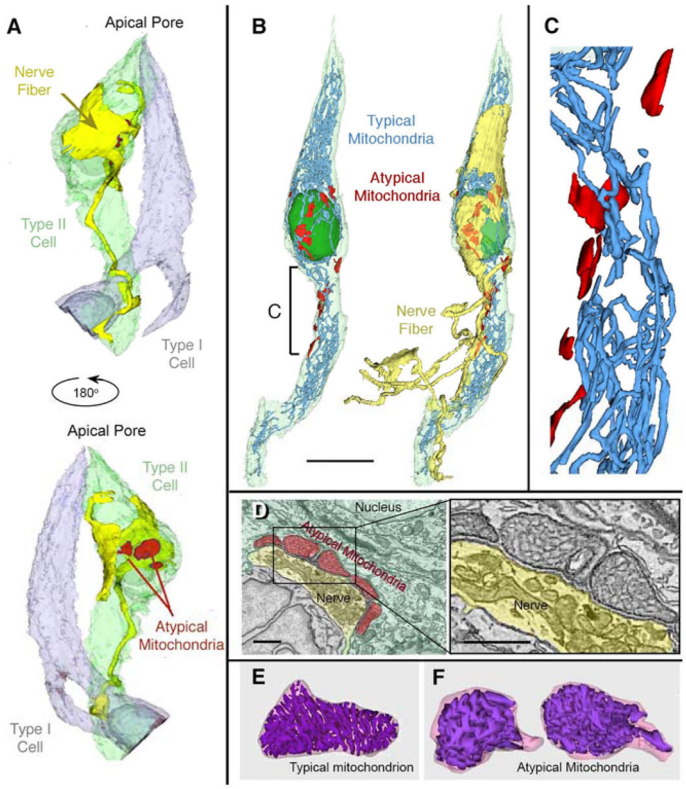

Figure 4. Reconstructions of typical mitochondria from sbfSEM data

(**A** & **A′**) Type II taste cell (green), a nerve fiber (yellow) and a Type I cell (gray) showing the relationship of atypical mitochondria (red) and sensory nerve fibers. A–B. Atypical mitochondria, rendered in red, appear only in areas of the taste cell facing the innervating nerve fiber. See Supplementary Video 1. (**B & B′**) Reconstruction of a Type II taste cell (pale green; nucleus dark green) showing typical (blue) and atypical mitochondria (red) in relation to the sensory nerve fiber (yellow in **B′**). Scale Bar = 10 μm. See also Supplementary Video 2. (**C**) Enlarged region from panel B, showing separation of atypical (red) from typical mitochondria (blue). Scale bar in Panel B = 3.82 μm as applied to **C**. See Supplementary Video 3. (**D**) Single image from a sbfSEM data set showing atypical mitochondria (pseudocolored red) and the afferent nerve terminal (yellow). Boxed area enlarged at right showing the tubular cristae within the atypical mitochondria. Scale bars = 1 μm. **E & F**. 3-D reconstructions of typical (**E**) and atypical (**F**) mitochondria (same pair as in Panel D). See also Suppl. Video 4.

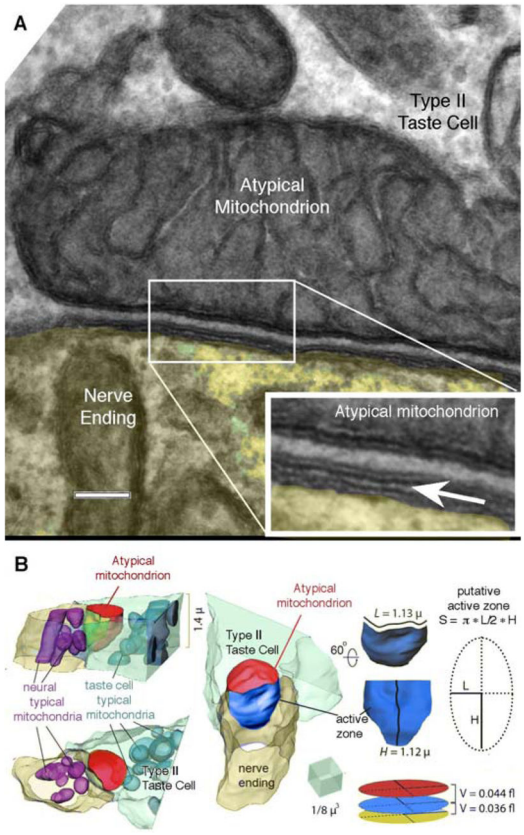

Fig. 5. Cell membrane specialization at the CALHM1-mitochondrial complex

(**A**) Conventional transmission electron micrograph illustrating the relationship between the membrane of the atypical mitochondrion, the plasma membrane of the taste cells and the nerve ending. Inset at lower right is an enlargement of the boxed area in the main image. The insert has been enlarged (3x) and the edges enhanced by application of an Unsharp Mask filter (60% @ 5 pixels). The arrow points to the synaptic cleft between the taste cell and nerve fiber. The uniform spacing between the mitochondrial outer membrane and the plasma membrane strongly suggests the presence of a scaffolding to maintain this relationship. Scale bar = 100 nm for the main image and 33.3 nm for the inset. **(B)** 3D reconstruction of a contact between Type II taste cell and the nerve ending (yellow) including visualizations of conventional mitochondria in the nerve ending (magenta), and an atypical mitochondrion (red) and conventional mitochondria (cyan) inside the taste cell (green). Note putative sub-mitochondrial active zone highlighted in blue. Detail to the right shows the method for approximating the volume of the different synaptic compartments.

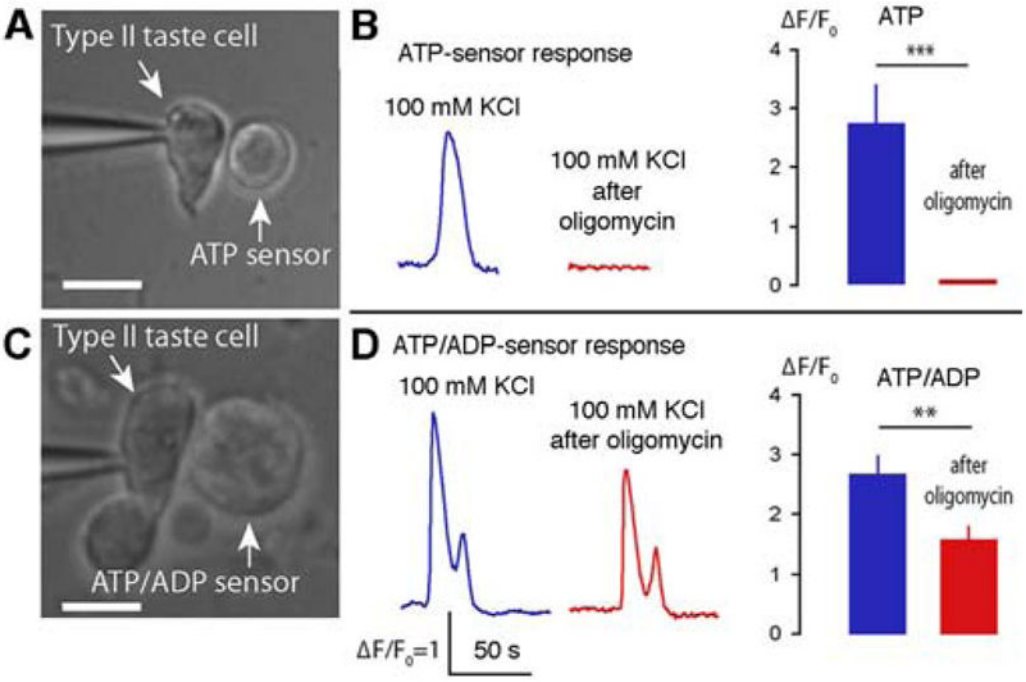

Fig. 6. Blocking ATP production in mitochondria blocks release of ATP

Oligomycin blocks ATP synthase in mitochondria allowing for the build-up of ADP within the matrix and intermembrane spaces. **(A)** ATP biosensor cells were transfected with mRNAs encoding P2X2/P2X3 ionotropic purinergic receptors, which are responsive to ATP but not ADP. **(B)** Before application of oligomycin, taste cells show a robust and repeatable release of ATP (blue trace). Five minutes after application of oligomycin, depolarization-evoked ATP release was eliminated (red trace). The bar graph shows a quantitative comparison of the responses (5 minutes with oligomycin, n=4, mean±SEM, P<0.001). **(C)** COS1 cells endogenously express P2Y receptors leaving them responsive to both ATP and ADP. **(D)** The response of the COS1 cells after oligomycin treatment (red trace in D) is attributable entirely to ADP rather than ATP since transfected ATP sensor CHO cells (B) show no ATP response. The bar graph shows a quantitative comparison of the responses (5 minutes with oligomycin, mean ± SEM. n=6, t-test ***P<0.001, **P<0.01). Scale bars in (A & C) are 10 μm. Validation of biosensor sensitivity and functionality in the presence of oligomycin are given in Supplementary Fig. 2.

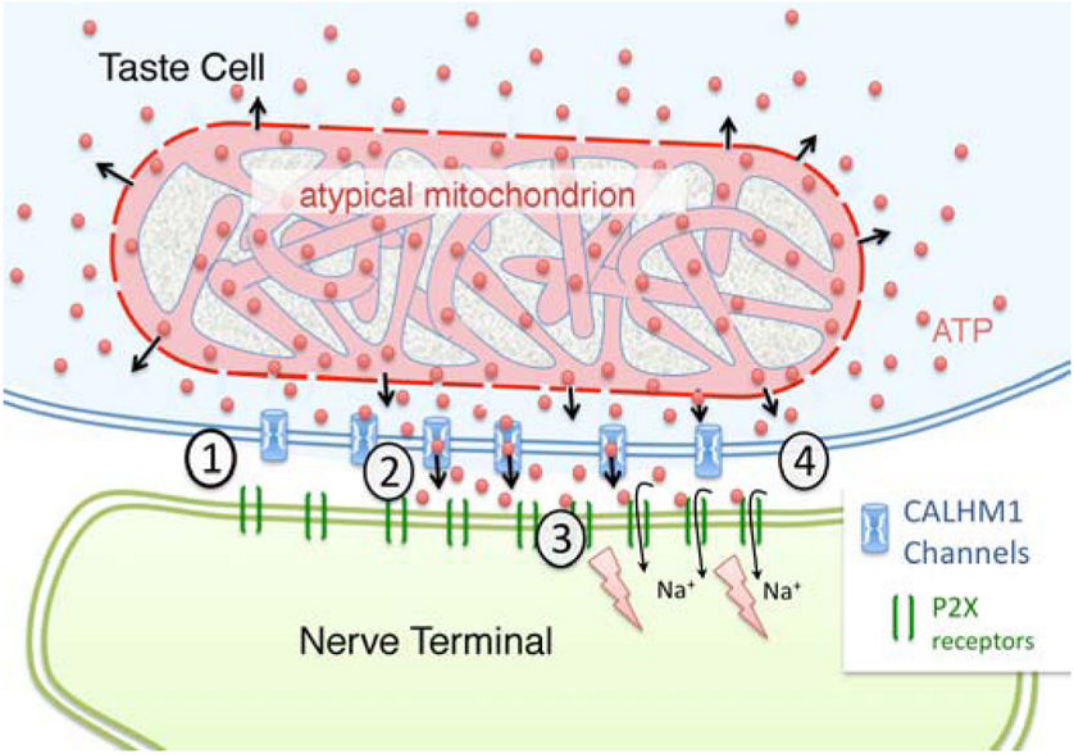

Fig. 7. Schematic diagram of a mitochondrial/CALHM1 synapse between a Type II taste cell (pale blue) and an afferent nerve terminal (green)

The CALHM1 channels lie within the plasma membrane of the taste cell between the atypical mitochondrion (pink) and the nerve terminal. In the resting state **(1),** CAHLM1 channels (Blue) are closed and ATP levels in the presynaptic compartment will be close to levels in the intermembrane space of the mitochondrion due to diffusion of ATP (red balls) through the porin channels of the outer mitochondrial membrane. Taste evoked action potentials in the taste cell open the CALHM1 channels (**2**) allowing ATP to flow into the synaptic cleft between the taste cell and the afferent nerve terminal. (**3**) The ATP in the intercellular space binds to and gates open the P2X receptors (green bars) in the neural membrane, permitting influx of sodium ions (Na^+) which depolarizes the afferent terminal. (**4**) As the taste cell repolarizes, CALHM1 channels close and extracellular levels of ATP return to pre-stimulus levels.

Table 1

Measurements of mitochondrial features comparing typical and atypical mitochondria in 3 different general size classes: small, medium, large

	Intermembrane space	Crista walls	Circumference	Enclosed area (ECSA)	Intermembrane space/total ECSA	Crista walls/total ECSA
SMALL						
Atypical	2,737±396.5	843.0±107.7	410.0±41.6	6,765±647	0.39±0.03	0.12±0.01
Typical	796.0±154.5	595.0±87.0	578.9±33.1	7,067±595	0.11±0.01	0.08±0.01
MEDIUM						
Atypical	4,885±352.6	1,736±80.7	653.9±31.8	13,213±550.5	0.37±0.03	0.13±0.01
Typical	1,385±169.3	1,323±149.3	701.4±48.0	10,865±925.1	0.12±0.01	0.12±0.01
LARGE						
Atypical	13,900±2,191.3	3,550±549.1	1044.2±91.5	33,654±5,570.5	0.42±0.03	0.11±0.01
Typical	2,536±446.6	2,193±307.9	1,408.6±101.8	22,675±1,981.8	0.11±0.01	0.09±0.01